

ELECTRONIC SUPPLEMENTARY INFORMATION

Light-triggered molecular switch for efficient OFET-based organic memory

Alexander V. Mumyatov,^a Lyubov A. Frolova,^a Lavrenty G. Gutsev,^a Ekaterina A. Khakina,^b Natalia A. Sanina,^a Sergey M. Aldoshin^a and Pavel A. Troshin^{*a}

^a Federal Research Center of Problems of Chemical Physics and Medicinal Chemistry of the Russian Academy of Sciences, Academician Semenov Avenue 1, Chernogolovka, Moscow Region, 142432, Russian Federation. E mail: troshin2003@inbox.ru, troshin@icp.ac.ru

^b A.N. Nesmeyanov Institute of Organoelement Compounds of Russian Academy of Sciences, Vavilova St. 28, bld. 1, Moscow, 119334, Russian Federation.

Instrumentation

Absorption spectra were measured on an Avantes AvaSpec-2048 optical fiber spectrometer. ¹H NMR spectra were obtained using a Bruker AVANCE 500 instrument. The transistor characteristics were measured using a Keithley 2612A dual-channel voltage and current source-meter. The devices were irradiated with a semiconductor laser modulated using an Advantest R6240A single-channel source-meter. Scanning electron microscopy images were obtained on a Zeiss SUPRA 25 instrument (Carl Zeiss Industrielle Messtechnik GmbH, Oberkochen, Germany). The capacitance of the dielectrics was measured by Aktakom AM-3125 RLC meter at frequency 100 kHz.

Fabrication and characterization of the memory device

Glass substrates (cover slips 1.5x1.5 cm in size) were cleaned for 5 min under the action of air plasma. Aluminum electrodes (gate) 100 nm thick were deposited onto the cleaned glass substrates by thermal evaporating in high vacuum (10^{-6} mbar) using a shadow mask. Electrochemical oxidation of aluminum gates for 360 s at a voltage of 30 V in a solution of citric acid (in a concentration of 2.8 g of citric acid per 50 mL of distilled water) was used to form the oxide layer of the dielectric. Thin films of photoactive spiropyran salt **SP/MC** were deposited over the dielectric inside the MBraun glove box under nitrogen (H_2O , $\text{O}_2 < 0.1$ ppm) by spin-coating from solutions in dimethylacetamide (10 mg mL^{-1}) at a substrate rotation speed of 750 rpm. Thus, the hybrid dielectric layer in the memory devices was an aluminum oxide film (20 nm) coated with **SP/MC** (20 nm). Next, a layer of the n-type semiconductor material (fullerene C_{60}) was deposited on the hybrid dielectric layer by resistive thermal evaporation in high vacuum (10^{-6} mbar) using a shadow mask (50 nm). The manufacture of the devices was completed by sputtering electrodes (drain and source) from silver under similar conditions. The transistor channel length (L) was 50 μm , and the width (W) was 2 mm. The capacitance of AlO_x and $\text{AlO}_x/\text{SP/MC}$ layers were 4.53×10^{-8} and $5.45 \times 10^{-9} \text{ F cm}^{-2}$, respectively.

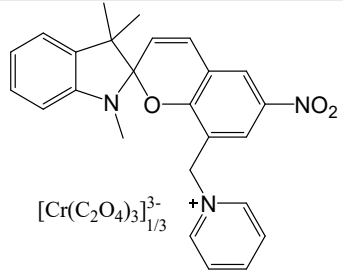
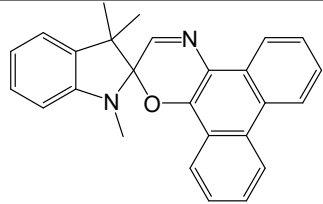
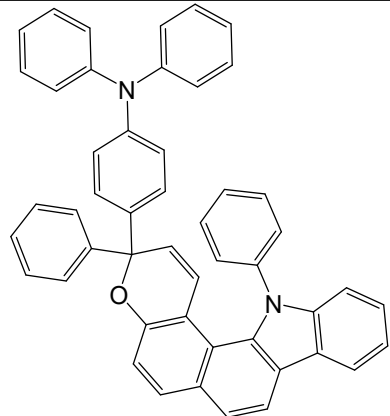
The memory devices were programmed by applying a voltage (V_p) between the source and gate and simultaneously irradiating the transistor channel with a diode laser light pulse ($\lambda = 405 \text{ nm}$, light intensity $\sim 60 \text{ mW cm}^{-2}$). Also, a green diode laser ($\lambda = 532 \text{ nm}$, light intensity $\sim 60 \text{ mW cm}^{-2}$) was used for optical programming of the devices. The transistor characteristics were measured using a Keithley 2612A dual-channel voltage and current source-meter. The devices were

irradiated with a semiconductor laser modulated using an Advantest R6240A single-channel source-meter.

DFT calculations

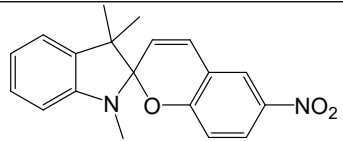
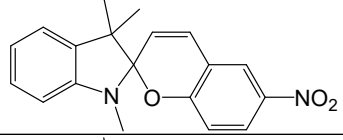
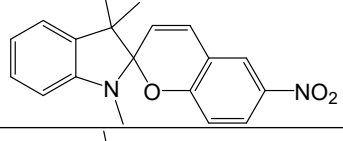
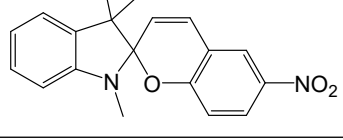
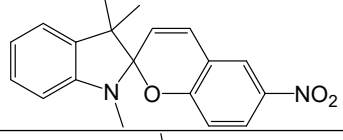
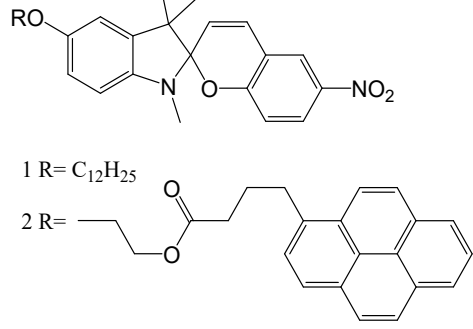
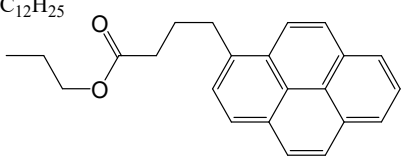
Our spin-polarized DFT calculations were performed using the GAUSSIAN 09 suite of programs [S1]. Initial relaxations were performed with the Gaussian 3-21G* basis set and the B3PW91 functional then the basis sets were improved to the triple- ζ quality 6-311+G* basis set and a single point calculation was done with the B3LYP functional. Where convergence was difficult, Gaussian's orbital shifting option was applied until convergence was achieved. The RMS force threshold was set to $3 \times 10^{-4} \text{ eV/\AA}$ and the total energy threshold to 10^{-8} a.u. Excited state properties were calculated with TDDFT. Local total spin magnetic moments on atoms were obtained using the natural atomic orbital populations (NAO) from the NBO analysis [S2]. Spin states were considered by optimizing the $2S+1=4$ quartet state for each configuration and then using the optimized MO coefficients and geometry as the guess configurations for $2S+1=2$ (spin flip down) and $2S+1=6$ (spin flip up). The calculated T_1 states shown in Figure S11 are adiabatic. Also, to ensure the Figure S11 results are consistent with experiment, we also calculated spiropyran and merocyanine as they are in the crystal (Figure 5) but with a Cl⁻ group to charge balance the pyridine ligand (Figure S12). In this case, we found that the adiabatic T_1 energies are essentially the same & thus the pyridine group does not appear to affect this aspect of the chemistry.

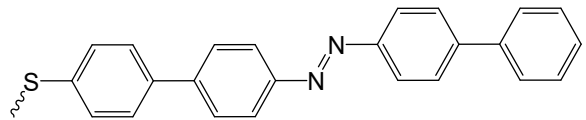
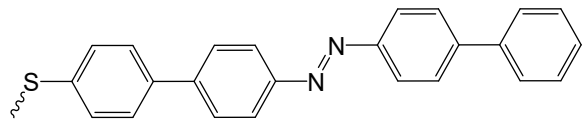
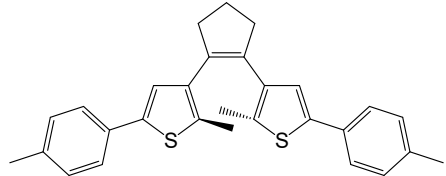
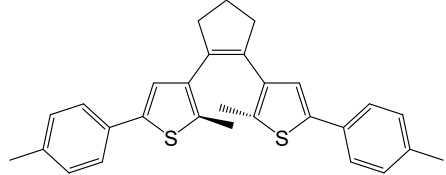
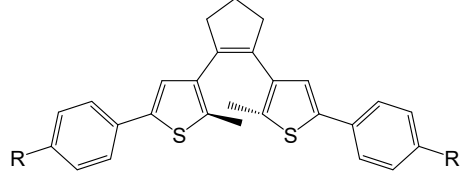
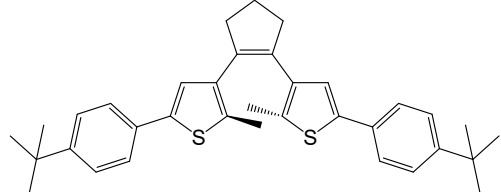
Table S1. An overview of the previously published results obtained using different types of molecules as optical switchers in OFETs.

Entry	Photochromic material	Operating voltage, V	Switching time	Switching coefficient $K_{SW}=I_{DS}(\text{state1})/$ $I_{DS}(\text{state2})$	Switching conditions	Ref.
0		-7 - +4	20 - 40 s	65	UV (F) VIS (B)	This work
1		-1 - +3	~1 min	~20	UV (F) VIS (B)	[S3]
2		~30	~30 min	~1.2	UV (F) VIS (B)	[S4]

ARTICLE

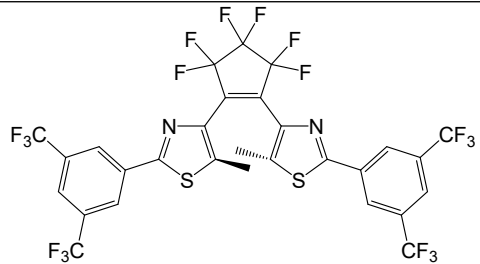
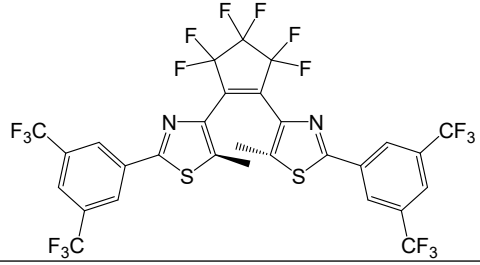
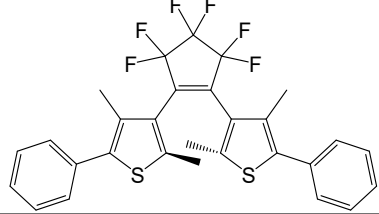
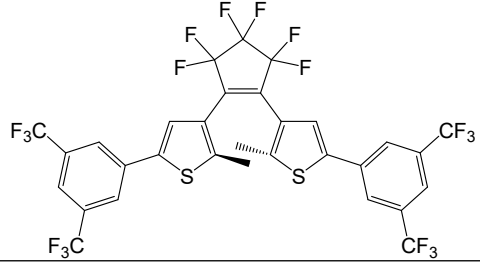
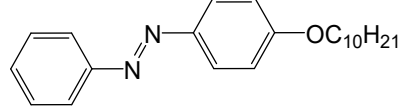
Journal Name

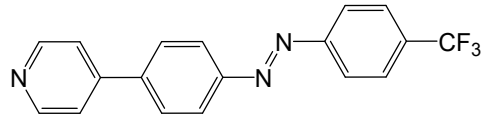
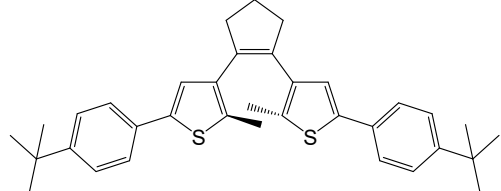
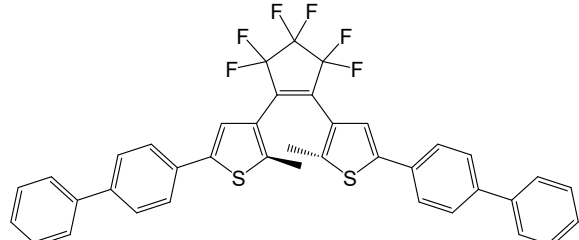
3		~50	~30 min	~1.8	UV (F) VIS (B)	[S5]
4		~60	~200 s	~1.002	UV (F) VIS (B)	[S6]
5		~50	10 - 1200 s	~1.03-3.0	UV (F) VIS (B)	[S7]
6		5-30	~10 - 40 s ~200 - 600 s	~1.3 ~2.0	UV (F) VIS (B)	[S8]
7		~100	~200 s	~1.06	UV (F) VIS (B)	[S9]
8	 <p>1 R = C₁₂H₂₅ 2 R = </p>	~8	~800 s	~2.6	UV (F) VIS (B)	[S10]

11		~30	~5 – 10 min	~6-13	UV (F) VIS (B)	[S11]
12		~80	~15 min	~3	UV (F) VIS (B)	[S12]
13		-40 - +40	2-12 min	1.2-10	UV (F) VIS (B)	[S13]
14		+40 - -60	5-10 min	~2.8	UV (F) VIS (B)	[S14]
15	 1 R= CH ₃ 2 R= CO ₂ -n-C ₆ H ₁₃	~100	~5 s	~1.2	UV (F) VIS (B)	[S15]
17		50 - 80	10 s	5-10	UV (F) VIS (B)	[S16]

ARTICLE

Journal Name

18		-30 - +30	16 – 30 s	~2.5	UV (F) VIS (B)	[S17]
19		80 - 120	30 s – 10 min	~2	UV (F) VIS (B)	[S18]
22		~90	~60 s	~6	UV (F) VIS (B)	[S19]
20		80 - 120	30 s – 10 min	~0.2	UV (F) VIS (B)	[S20]
10		-60 - +60	10 – 50 s	~450	UV (F) VIS (B)	[S21]

9		+60 - -60	10 min -1 h	$\sim 10^2$ - 10^3	UV (F) VIS (B)	[S22]
16		+50 - -60	30 s - 5 min	$\sim 10^2$ - 10^3	UV (F) VIS (B)	[S23]
21		-20 - -100	2 - 3 min	$\sim 10^2$	UV (F) VIS (B)	[S24]

F - corresponds to forward switching

B - corresponds to the backward transition

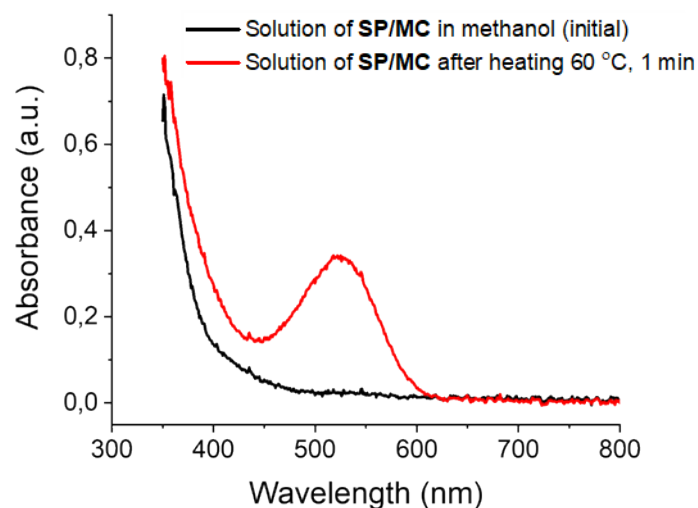


Fig. S1 - Absorption spectra of a methanolic solution of **SP/MC** in the pristine (initial) state and after heating at 60 °C for 1 min.

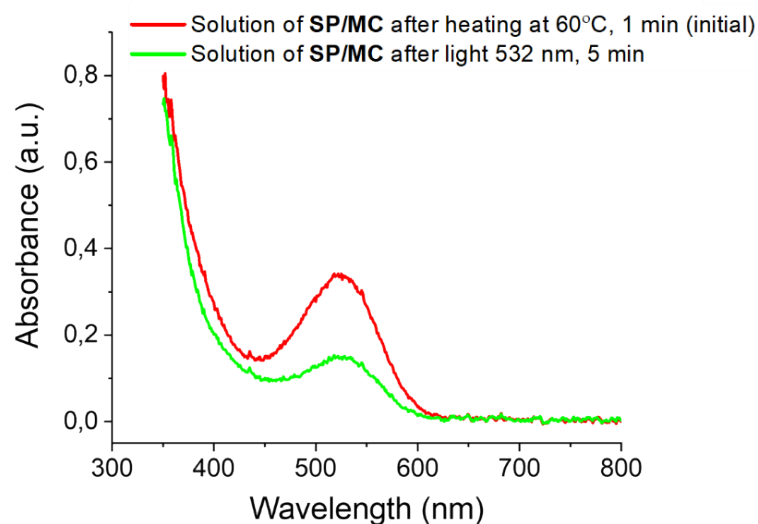


Fig. S2 - Absorption spectra of a methanolic solution of **SP/MC** after heating at 60 °C for 1 min: initial state, after illumination with the green light ($\lambda = 532$ nm) for 5 min.

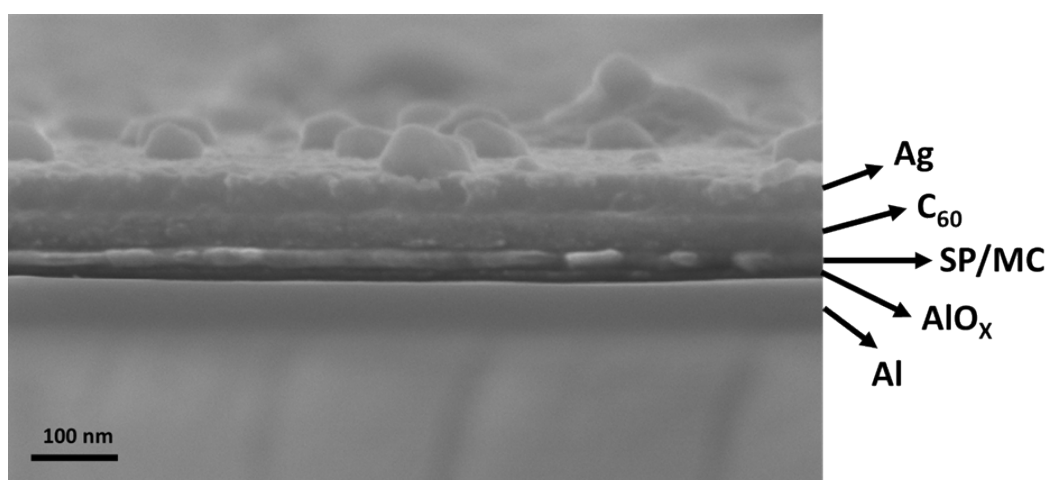


Fig. S3 - Cross-sectional SEM image of the OFET

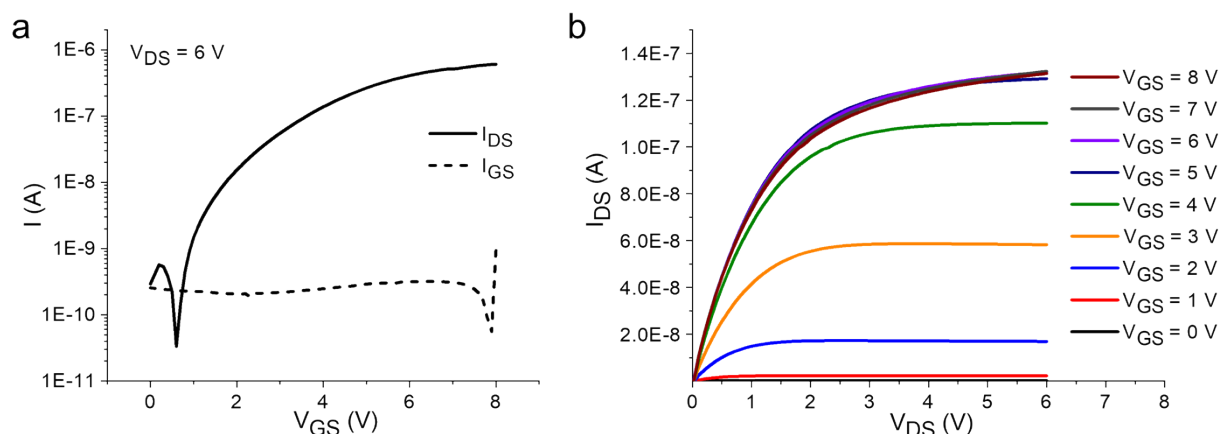


Fig. S4 - Initial transfer (a) and output (b) characteristics of memory elements based on OFETs with spiropyran salt **SP/MC**.

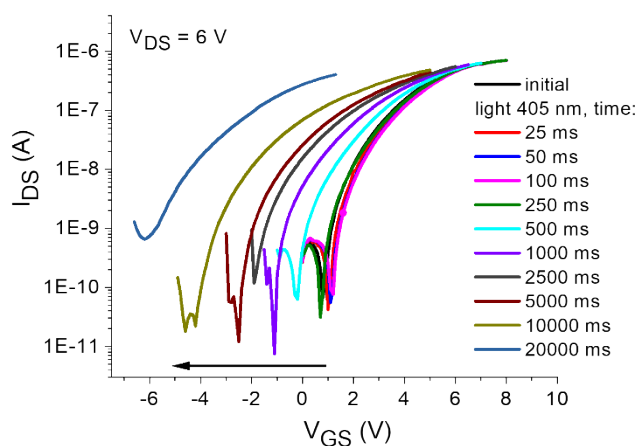


Fig. S5 - Evolution of the transfer characteristics of the devices comprising **SP/MC** under violet light ($\lambda = 405$ nm) as a function of the programming time.

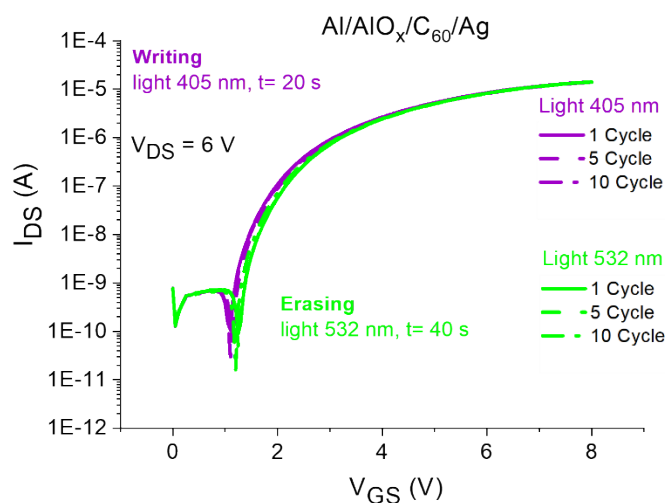


Fig. S6 - The evolution of the transfer characteristics of the OFET without spiropyran **SP/MC** interlayer upon exposure to violet or green light (405 nm or 532 nm).

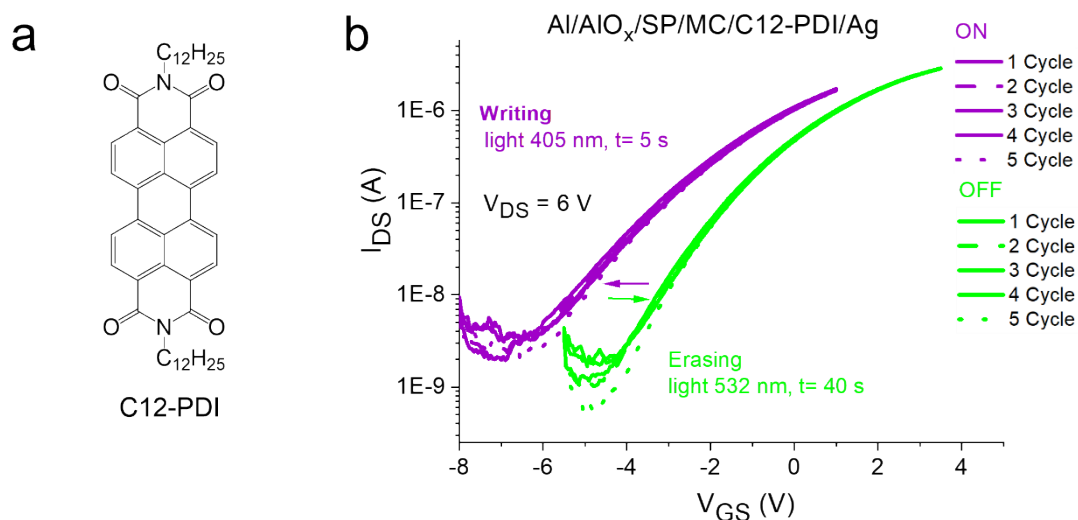


Fig. S7 – Molecular structure of C12-PDI semiconductor material (a) and optical switching of the OFET-based memory devices with spiropyran **SP/MC** interlayer and C12-PDI semiconductor under exposure to violet or green light (405 nm or 532 nm) (b)

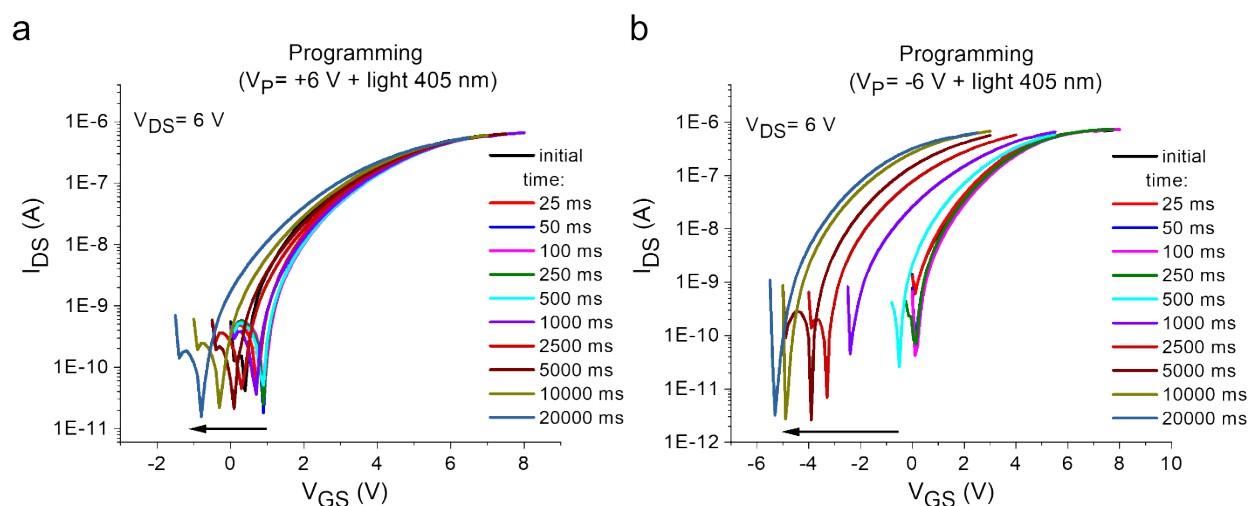


Fig. S8 - Evolution of the transfer characteristics of the devices comprising **SP/MC** under a positive applied voltage ($V_P = 6\text{ V}$) (a) and negative applied voltage ($V_P = -6\text{ V}$) (b) and violet light ($\lambda = 405\text{ nm}$) as a function of the programming time.

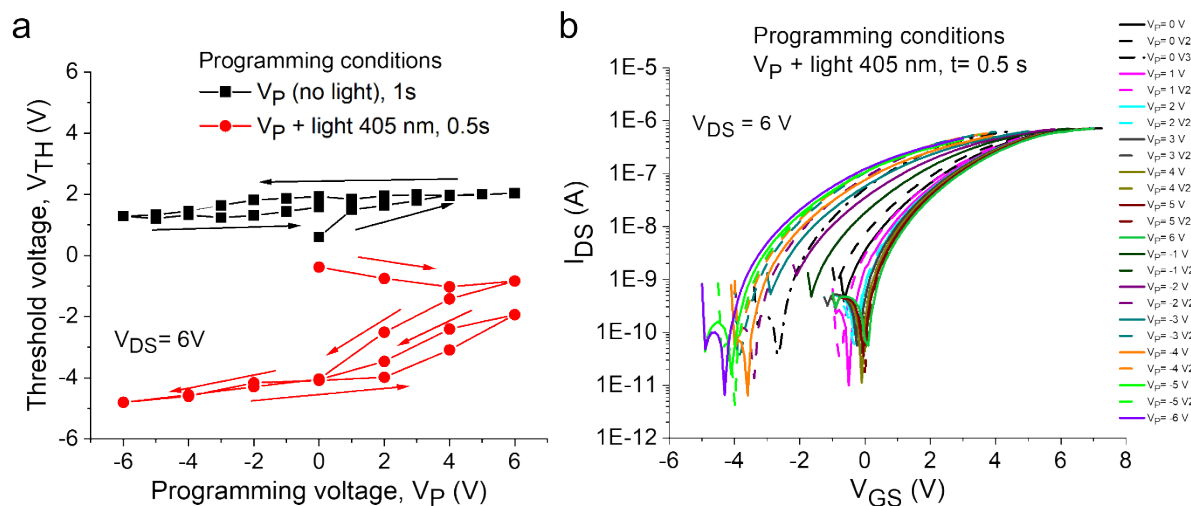


Fig. S9 - Evolution of the OFET threshold voltage as a function of the programming voltage for devices comprising **SP-1** (a) and transfer characteristics of the devices obtained under different programming voltages (b).

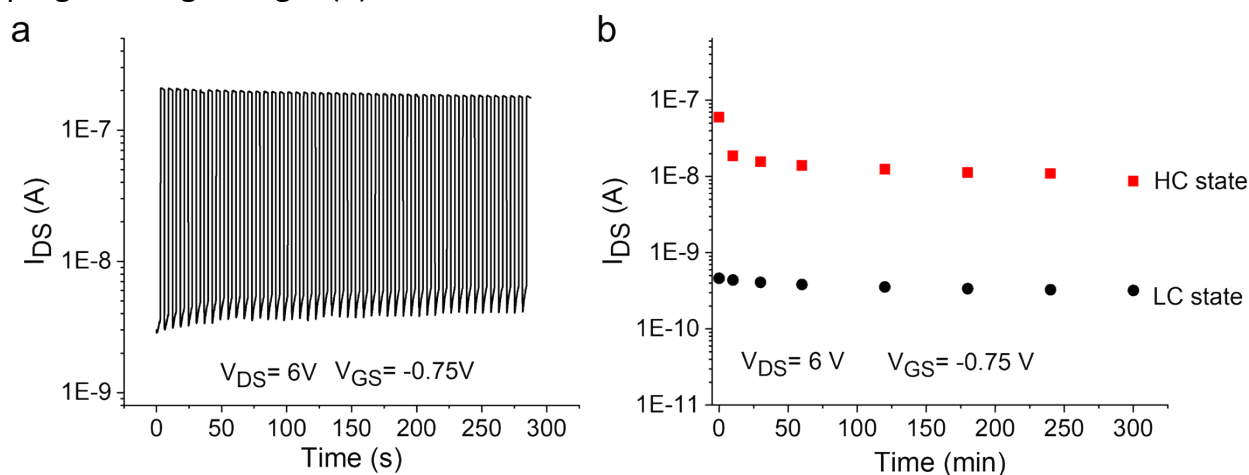


Fig. S10 - Forty-five manually recorded write-read-erase cycles for one of the devices (a) and retention characteristics of the device in “HC” and “LC” states (b). In both cases, the devices were programmed by simultaneous applying of electric bias V_P and violet light.

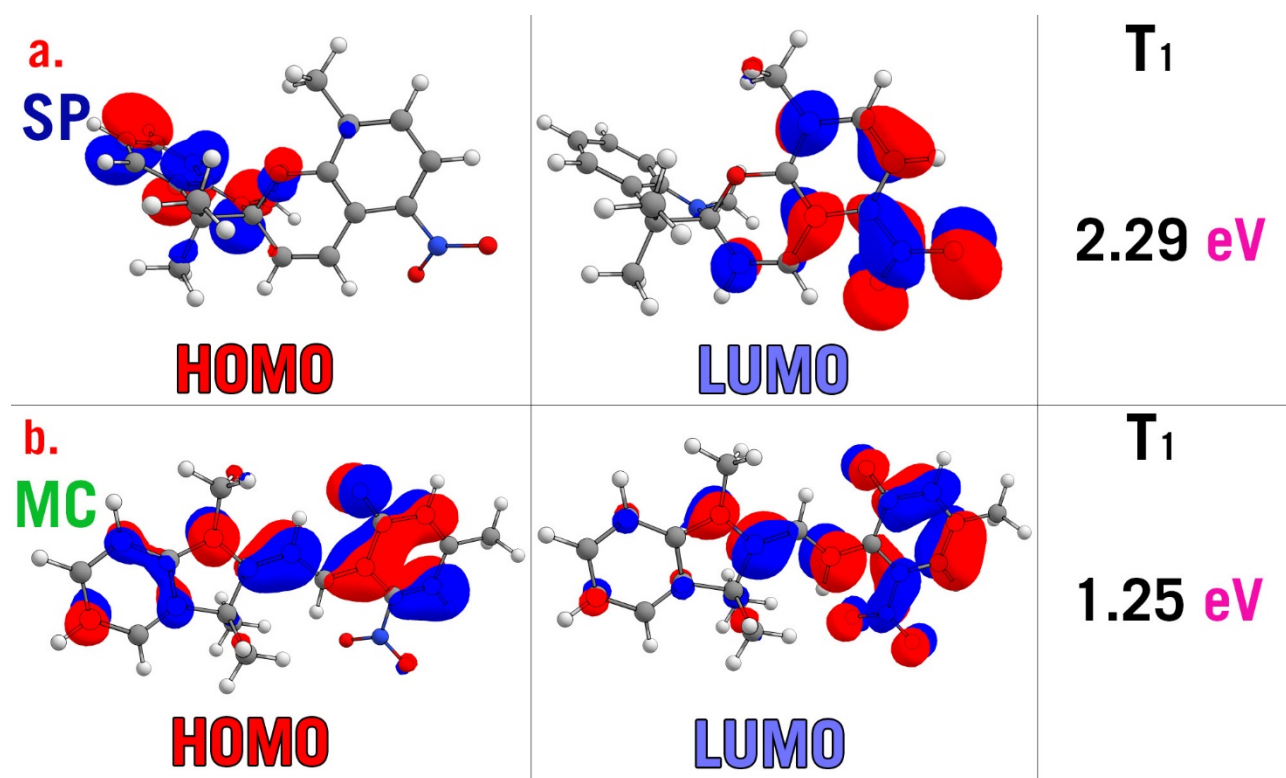


Fig. S11 - The HOMO, LUMO and T₁ energies of a. spirocyanine (top row) and b. merocyanine (bottom row).

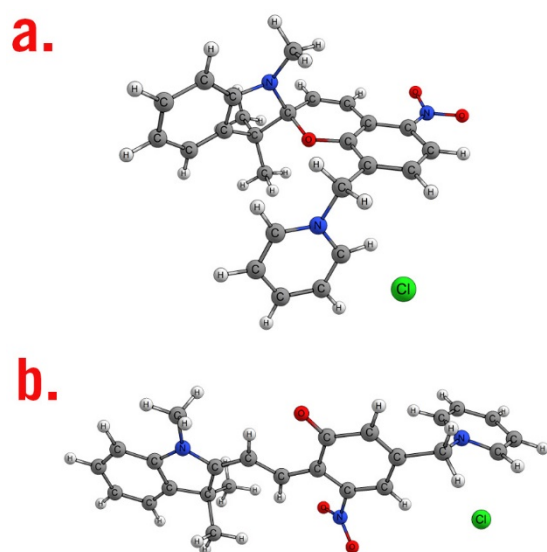


Fig. S12 - The a. spirocyanine and b. merocyanine with a charge balanced pyridine-Cl group attached.

References

1. Robert, M. Affinité de l'hémoglobine pour l'oxygène. *Bulletin de physio-pathologie respiratoire* 1975, **11**, 79–170
2. Glendening, E. D., Reed, A. E., Carpenter, J. E. & Weinhold, F. NBO 3.0. *QCPE Bull.* 1990, **10**,
3. L. A. Frolova, P. A. Troshin, D. K. Susarova, A. V. Kulikov, N. A. Sanina and S. M. Aldoshin, *Chem. Commun.*, 2015, **51**, 6130–6132.
4. Y. Ishiguro, M. Frigoli, R. Hayakawa, T. Chikyow and Y. Wakayama, *Organic Electronics*, 2014, **15**, 1891–1895.
5. Y. Ishiguro, R. Hayakawa, T. Chikyow and Y. Wakayama, *J. Mater. Chem. C*, 2013, **1**, 3012.
6. Y. Li, H. Zhang, C. Qi and X. Guo, *J. Mater. Chem.*, 2012, **22**, 4261–4265.
7. H. Zhang, X. Guo, J. Hui, S. Hu, W. Xu and D. Zhu, *Nano Lett.*, 2011, **11**, 4939–4946.
8. Q. Shen, L. Wang, S. Liu, Y. Cao, L. Gan, X. Guo, M. L. Steigerwald, Z. Shuai, Z. Liu and C. Nuckolls, *Adv. Mater.*, 2010, **22**, 3282–3287.
9. Q. Shen, Y. Cao, S. Liu, M. L. Steigerwald and X. Guo, *J. Phys. Chem. C*, 2009, **113**, 10807–10812.
10. X. Guo, L. Huang, S. O'Brien, P. Kim and C. Nuckolls, *J. Am. Chem. Soc.*, 2005, **127**, 15045–15047.
11. C. Raimondo, N. Crivillers, F. Reinders, F. Sander, M. Mayor and P. Samorì, *Proc. Natl. Acad. Sci. U.S.A.*, 2012, **109**, 12375–12380.
12. N. Crivillers, E. Orgiu, F. Reinders, M. Mayor and P. Samorì, *Adv. Mater.*, 2011, **23**, 1447–1452.
13. M. Carroli, A. G. Dixon, M. Herder, E. Pavlica, S. Hecht, G. Bratina, E. Orgiu and P. Samorì, *Adv. Mater.*, 2021, **33**, 2007965.
14. M. Carroli, D. T. Duong, E. Buchaca-Domingo, A. Liscio, K. Börjesson, M. Herder, V. Palermo, S. Hecht, N. Stingelin, A. Salleo, E. Orgiu and P. Samorì, *Adv. Funct. Mater.*, 2020, **30**, 1907507.
15. E. Orgiu, N. Crivillers, M. Herder, L. Grubert, M. Pätzelt, J. Frisch, E. Pavlica, D. T. Duong, G. Bratina, A. Salleo, N. Koch, S. Hecht and P. Samorì, *Nature Chem*, 2012, **4**, 675–679.
16. M. E. Gemayel, K. Börjesson, M. Herder, D. T. Duong, J. A. Hutchison, C. Ruzié, G. Schweicher, A. Salleo, Y. Geerts, S. Hecht, E. Orgiu and P. Samorì, *Nat Commun*, 2015, **6**, 6330.
17. H. Qiu, Y. Zhao, Z. Liu, M. Herder, S. Hecht and P. Samorì, *Adv. Mater.*, 2019, **31**, 1903402.
18. K. Börjesson, M. Herder, L. Grubert, D. T. Duong, A. Salleo, S. Hecht, E. Orgiu and P. Samorì, *J. Mater. Chem. C*, 2015, **3**, 4156–4161.
19. M. Yoshida, K. Suemori, S. Uemura, S. Hoshino, N. Takada, T. Kodzasa and T. Kamata, *Jpn. J. Appl. Phys.*, 2010, **49**, 04DK09.
20. K. Börjesson, M. Herder, L. Grubert, D. T. Duong, A. Salleo, S. Hecht, E. Orgiu and P. Samorì, *J. Mater. Chem. C*, 2015, **3**, 4156–4161.
21. Y. Zhao, S. Bertolazzi and P. Samorì, *ACS Nano*, 2019, **13**, 4814–4825.
22. Y. Wang, D. Iglesias, S. M. Gali, D. Beljonne and P. Samorì, *ACS Nano*, 2021, **15**, 13732–13741.
23. L. Hou, T. Leydecker, X. Zhang, W. Rekab, M. Herder, C. Cendra, S. Hecht, I. McCulloch, A. Salleo, E. Orgiu and P. Samorì, *J. Am. Chem. Soc.*, 2020, **142**, 11050–11059.
24. R. Hayakawa, K. Higashiguchi, K. Matsuda, T. Chikyow and Y. Wakayama, *ACS Appl. Mater. Interfaces*, 2013, **5**, 3625–3630.